

1 **Fate of sulfamethoxazole in groundwater: conceptualizing and modeling**
2 **metabolite formation under different redox conditions**

3 Paula Rodríguez-Escales*, Xavier Sanchez-Vila

4 Hydrogeology Group (UPC-CSIC), Dept. of Civil and Environmental Engineering. Universitat Politècnica de Catalunya,
5 Jordi Girona 1-3, 08034 Barcelona, Spain

6 *Corresponding author: paula.rodriguez.escales@upc.edu

7

8 **ABSTRACT**

9 Degradation of emerging organic compounds in saturated porous media is usually postulated
10 as following simple low-order models. This is a strongly oversimplified, and in some cases
11 plainly incorrect model, that does not consider the fate of the different metabolites.
12 Furthermore, it does not account for the reversibility in the reaction observed in a few
13 emerging organic compounds, where the parent is recovered from the metabolite. One such
14 compound is the antibiotic sulfamethoxazole (SMX). In this paper, we first compile existing
15 experimental data to formulate a complete model for the degradation of SMX in aquifers
16 subject to varying redox conditions, ranging from aerobic to iron reducing. SMX degrades
17 reversibly or irreversibly to a number of metabolites that are specific of the redox state.
18 Reactions are in all cases biologically mediated. We then propose a mathematical model that
19 reproduces the full fate of dissolved SMX subject to anaerobic conditions and that can be used
20 as a first step in emerging compound degradation modeling efforts. The model presented is
21 tested against the results of the batch experiments of Barbieri et al. (2012) and Nödler et al.
22 (2012) displaying a non-monotonic concentration of SMX as a function of time under
23 denitrification conditions, as well as those of Mohatt et al. (2011), under iron reducing
24 conditions.

25

26 **Keywords**

27 Sulfamethoxazole, denitrification, oxidation-reduction, co-metabolism, metabolites, modeling

28

29 **1 Introduction**

30 The presence of pharmaceutical compounds in aquatic environments has been frequently
31 addressed in recent years, and it is the topic of numerous review articles (Gavrilescu et al.
32 2015, Schwarzenbach et al. 2006). The discharge of antibiotics into the environment has
33 become a major concern, as this group of pharmaceuticals is not only prone to directly
34 influencing microbial communities (Fent et al. 2006, Yan et al. 2013), but also because of the
35 risk of worldwide dispersal of antibiotic-resistant bacterial genes (Szczepanowski et al. 2009).
36 Antibiotics may enter the environmental system via wastewater or else as wastewater
37 treatment plant (WWTP) effluents, diffusive agricultural input (Jjemba 2002), or landfill
38 discharge (Heberer 2002), and they can be found in different environmental compartments
39 such as surface and subsurface water bodies, sediments, and soils.

40 Sulfamethoxazole (SMX) is a polar sulfonamide antibiotic, and the most widely detected
41 antibiotic in aquatic environments (Gao et al. 2014). SMX mainly enters wastewater via human
42 excretion either unmodified or as its human-metabolized transformation products, N-acetyl-
43 SMX or N-SMX-glucuronide (Göbel et al. 2005). Both transformation products are easily
44 cleaved back to the SMX parent compound (Göbel et al. 2005). Since SMX is not completely
45 degraded in wastewater treatment plants, it is found in minute concentrations in the WWTP
46 water effluents, eventually reaching soils and surface or subsurface water bodies. Actually, it
47 has been found in concentrations up to 0.47 µg/L in aquifers and 0.48 µg/L in surface waters
48 (Hirsch et al. 1999). SMX has a very low adsorptivity to most soils (Henzler et al. 2014, Schaffer
49 et al. 2015). Thus, it is postulated that sorption into aquifer sediments is usually negligible, so
50 that the observed reduction of concentrations of SMX in the environmental compartments is
51 mainly due to degradation.

52 In general, the literature on SMX degradation in both WWTPs and natural aqueous
53 environments is marked by inconsistent results. This is supposedly because elimination
54 amounts and rates depend on various environmental factors such as *in situ* redox potential,
55 available nutrients, soil characteristics, seasonal temperature, microbial adaptation, and light
56 variations (Müller et al. 2013), all such factors being site-dependent and temporally variable.

57 Based on field observations and laboratory experiments, it is postulated that degradation
58 of SMX is biologically mediated and occurs preferentially under strictly anaerobic conditions
59 (Banzhaf et al. 2012, Grünheid et al. 2005, Heberer et al. 2008, Schaffer et al. 2015, Valhondo
60 et al. 2015). Some lab experiments reported the fate of SMX for particular redox conditions
61 such as denitrification (e.g., Barbieri et al. 2012, Nödler et al. 2012) or iron reducing conditions
62 (e.g., Mohatt et al., 2011). Nevertheless, aerobic degradation of SMX has also been observed
63 in aerobic environments such as activated sludge (Baumgarten et al. 2011, Drillia et al. 2005,
64 Gauthier et al. 2010, Reis et al. 2014).

65 Besides biological processes, abiotic SMX elimination has also been reported. For
66 example, chemical oxidation was found to be an effective degradation process by using
67 persulfate in the presence of ferrous iron oxidizing to ferric iron (Ji et al. 2014). The
68 complementary mechanism was described in Mohatt et al. (2011), where abiotic degradation
69 was enhanced by the biological reduction of ferric iron into ferrous iron.

70 Only in experiments performed under either aerobic conditions sustained for large times
71 (Müller et al. 2013, Reis et al. 2014) or in anaerobic iron reducing conditions (Mohatt et al.
72 2011), the irreversible breakage of the SMX molecule was observed. Contrarily, the
73 metabolites observed during denitrification conditions resulted from the substitution of the
74 primary amine of SMX, forming either 4-nitro-SMX or else desamino-SMX (Barbieri et al. 2012,
75 Nödler et al. 2012). In these last two papers, the authors reported that metabolites were not
76 stable, meaning that when the denitrification process was over they were retransformed into
77 the parent compound (see also Banzhaf et al. 2012).

78 Despite all the existing literature dealing with the fate of SMX under different redox
79 conditions, there is little work postulating the processes taking place at the molecular scale,
80 proposing closed-form expression for reaction rates, and reproducing the experimental
81 observations of SMX fate through mathematical modeling. According to Henzler et al. (2014),
82 this assertion is also valid for a large number of emerging organic compounds (EOCs). Most of
83 the published works assume that degradation can be explained by (apparent) first-order
84 degradation rates for all EOCs in a given cocktail (Henzler et al. 2014, Nham et al. 2015,
85 Schaffer et al. 2015). Only few studies have investigated quantitatively the actual processes
86 driven by varying redox conditions over degradation rates of EOCs (Greskowiak et al. 2006, Liu
87 et al. 2013). Moreover, this simplified approach, based on first-order reactions, accounts only
88 for the presence of irreversible reactions, contradicting a number of experiments where
89 reversibility of the transformation processes has been observed (Barbieri et al. 2012, Stadler et
90 al. 2015). While it is obvious that each antibiotic displays an individual, non-generalizable
91 degradation behavior, it is also true that understanding one of them will open the door to
92 analyze in the future the fate of a cocktail of antibiotics (and their metabolites), including also
93 potential synergies.

94 Considering all of this, the objective of this work was to develop a conceptualization of
95 the molecular mechanisms of degradation of the sulfamethoxazole molecule under different
96 redox conditions ranging from aerobic to iron-reducing conditions, and a mathematical model
97 capable of reproducing these mechanisms, with the overall aim of tracing the metabolite
98 formation from different degradation pathways. To our knowledge, this is the first work which
99 integrates all known processes on the degradation pathways of sulfamethoxazole as well as its
100 metabolites in groundwater and under different redox conditions in a consistent mathematical
101 framework that is able to describe various experimental data sets. To illustrate the conceptual
102 and mathematical work, we model and interpret three published experiments, two of them

103 performed under nitrate reducing conditions (Barbieri et al., 2012; Nödler et al., 2012), and
104 one under iron reducing ones (Mohatt et al., 2011).

105 **2 Methods**

106 **2.1 Observations and conceptualization of the molecular mechanisms**

107 The literature provides information regarding degradation of SMX only under aerobic and
108 partially under anaerobic (nitrate and iron reduction) conditions. Although in Mohatt et al.
109 (2011) SMX degradation under sulfate reduction condition was observed, to our knowledge,
110 no experimental information is available describing such process, and thus no metabolites
111 have been observed. So, in this work we conceptualize the SMX degradation for aerobic
112 conditions, denitrification, and iron reducing conditions.

113 **2.1.1 SMX behavior under aerobic conditions**

114 Aerobic degradation of SMX has been mostly studied in the context of WWTPs and surface
115 water bodies, and it is not expected to be a significant process in groundwater bodies due to
116 their generally low oxygen concentrations. Degradation has mostly been observed for large
117 SMX concentrations (Drillia et al. 2005) and with acclimated biomass in active sludge systems
118 (Müller et al. 2013, Reis et al. 2014). SMX degradation was observed either via direct
119 metabolism or else via co-metabolism (Gauthier et al., 2010; Reis et al., 2014; Drillia et al.,
120 2005); in the latter case, degradation rates were generally comparably larger. Additionally, one
121 study reported aerobic degradation of SMX in a column experiment supplied with surface
122 water (Baumgarten et al. 2011). The degradation was linked to large adaptation times, around
123 1 year for the degradation at the lowest concentration of SMX (0.25 µg/L) and 3-12 months for
124 the highest reported one (1.4 µg/L).

125 The most frequent metabolite produced under aerobic conditions was 3-amino-5-
126 methylisoxazole (Müller et al. 2013, Reis et al. 2014). This metabolite represents an irreversible
127 breakage of the SMX molecule, more precisely of the sulfonamide radical, in concordance with

128 the aerobic degradation pathway first predicted by Gao et al. (2010) (Figure 1). This pathway
129 would facilitate the complete mineralization of 4-aminobenzolsulfonate (a by-product of the
130 reaction), as this compound could also be degraded under aerobic conditions (Gao et al. 2010).

131 According to different authors (Baumgarten et al. 2011, Gauthier et al. 2010, Reis et al.
132 2014), aerobic degradation can be modeled as first-order kinetics. Table 1 shows a review of
133 the apparent half-lives for SMX degradation compiled from experiments available in the
134 literature. It is noticeable that all half-live values were determined whenever biomass was
135 completely acclimated; this would indicate that in more general systems, with no acclimated
136 biomass, real half-lives (if at all existing) would be larger.

137 **2.1.2 SMX behavior under nitrate reducing conditions**

138 As already presented in the introduction, SMX degradation under nitrate reducing conditions
139 has been widely reported. Because of the controlled conditions of the experiments and
140 metabolite monitoring we have focused our analysis in the works of Barbieri et al., 2012 (from
141 now on BAR) and Nödler et al., 2012 (denoted NDL in the sequel).

142 **2.1.2.1 Observations and process inference**

143 The BAR and NDL experiments were developed under identical experimental conditions,
144 involving sets of microcosms containing natural sediments, synthetic water and SMX (injected
145 in a cocktail of EOCs). They included a set of biotic and abiotic series by duplicate to separate
146 biodegradation (both biotic mineralization and transformation included here) from sorption or
147 other abiotic processes. The experiments were performed inside a glove box under Argon
148 atmosphere and into 0.3 L glass bottles running for 21 days in the BAR experiment and 90 days
149 for NDL. Bottles were filled with 0.24 L of water with the chemical signature provided in Table
150 2 and 120 g of air-dried and homogenized quaternary alluvial sediments composed by quartz,
151 calcite, albite, dolomite, clonochlore and illite in different proportions. The organic carbon and
152 the nitrogen present in the sediment were lower than 0.2% in mass. Mn and Fe (III) associated

153 to oxide-hydroxides and oxides were 0.007% for Mn and 0.584% for total Iron. Denitrification
154 conditions were stimulated by adding easily degradable organic compounds (sodium acetate
155 and methanol) to act as electron donors. Additional information and analytical details can be
156 found in Barbieri et al. (2012) and in Barbieri et al. (2011). Concurrently, a set of abiotic
157 experiments were performed with an identical full setup except that a small concentration of
158 HgCl_2 was added to the solution in order to inhibit biological activity.

159 The results of the biotic experiments showed a decrease in time of nitrate and organic
160 carbon after lag phases of 1.8 and 3 d in the BAR and NDL experiments, respectively (Figures
161 2a and 2d). The lag phase was attributed to an adaption period for the denitrifying bacteria. A
162 transient accumulation of nitrite taking place simultaneously with a decrease in nitrate was
163 observed in both experiments, indicating partial denitrification. After 10 days, nitrate and
164 nitrite were completely depleted in the BAR experiment. After that (between 10 and 21 days) a
165 small production of Mn^{+2} and Fe^{+2} was observed indicating a transition towards stronger
166 reducing conditions (lower Eh). On the other hand, in the NDL experiment denitrification was
167 active even after 90 days, with remaining concentrations of nitrate and nitrite of 3.5 and 0.16
168 mM, respectively, suggesting incomplete denitrification by the end of the experiment.

169 Almost full depletion of SMX was observed during the period corresponding to transient
170 accumulation of nitrite in both experiments (Figures 2b, 2e). During this time, the metabolite
171 4-nitro-SMX was detected and quantified in both experiments, whereas a second metabolite,
172 desamino-SMX, was also detected in NDL experiment (it was not monitored in BAR). After
173 denitrification was over (BAR) or close to being complete (NDL), the two metabolites were
174 virtually depleted in the system, while SMX reappeared, reaching concentration values of the
175 same order than the initial injected ones. At this point it is relevant to state that the NDL
176 experiment involved an initial concentration of SMX 1000 times larger than that of BAR (recall
177 Table 2), indicating that the process was not an artifact attributable to high or low input
178 concentrations.

179 Regarding the abiotic experiments, the concentration of SMX remained constant during
180 all the duration of the experiment indicating that SMX depletion in the biotic experiments was
181 driven by biological activity (Figures 2a-f).

182 Concerning the mass balance of SMX compounds, the BAR experiment showed a gap
183 during the denitrification phase, and by the end of the experiment the concentration of SMX
184 was about 75% of the initial value (Figure 2c). On the other hand, the mass balance in NDL had
185 a sudden decay of about 45% at the first sampling point (day 5) and from then on it remained
186 approximately constant until the end (day 90) of the experiment (Figure 2f). As experimental
187 conditions were similar in the two experiments, we assumed that the gap observed in the
188 mass balance of BAR could represent the formation of the desamino-SMX metabolite (not
189 measured). Thus, it seemed that a part of SMX disappeared in an unknown pathway when
190 denitrification started ($25\pm 5\%$ and $45\pm 2\%$ in the BAR and NDL experiments, respectively)
191 whereas the remainder was fully transformed into 4-nitro-SMX and desamino-SMX. These two
192 compounds were unstable metabolites that were re-transformed into SMX, the parent
193 compound, when nitrate and nitrite were (almost completely) depleted.

194 **2.1.2.2 Conceptualization**

195 The generation of the two metabolites 4-nitro-SMX and desamino-SMX in the BAR experiment
196 was ascribed to the denitrification activity enhanced by the presence of a large external source
197 of organic carbon. In both metabolites the key point is the substitution of the primary amine of
198 sulfamethoxazole by different radicals. The formation of 4-nitro-SMX implies the nitrosation of
199 the primary amine of SMX, whereas desamino-SMX involves the deamination process again of
200 the primary amine. From these considerations, we propose the next conceptual model
201 (summarized in Figure S1 of Supplementary Material).

202 The occurrence of either nitrosation or deamination of the primary amine could be
203 attributed to the presence of nitrous acid, the conjugate (weak) acid of nitrite (with $pK_a = 3.15$
204 at 25°C , see Morrisson and Boyd (1992)). The presence of nitrous acid facilitated the formation

205 of a diazonium cation replacing the amine radical in SMX. This compound was not stable under
206 ambient conditions and thus, could undergo numerous and consecutive fast reactions, strongly
207 depending on reaction conditions and available reaction partners (Carey and Sundberg 2007,
208 Morrisson and Boyd 1992). One reaction path consisted of the diazonium molecule reacting
209 again with another acid nitrous molecule forming 4-nitro-SMX. A second path implied the
210 reaction of the diazonium molecule with an alcohol (methanol was present in the batch
211 experiment), forming a desamino-SMX molecule (Everett 1973). All the reactions paths and the
212 molecules proposed are sketched in Figure S1 of Supplementary Material.

213 Note that the formation of 4-nitro-SMX and desamino-SMX were both driven by the
214 presence of HNO_2 , a subproduct of the denitrification process. Nevertheless, the reaction of
215 degradation of SMX was abiotic, meaning that SMX did not participate in the denitrifying
216 metabolism. Thus, the co-metabolic pathway of degradation consisted in the generation of
217 nitrite as an intermediate product of the denitrifying metabolism. At that point, nitrite was
218 conjugated with H^+ and formed HNO_2 which was the responsible to generate an abiotic
219 reaction with a diazonium salt as an intermediate product, and the last responsible of the
220 observed decay (and virtual disappearance) of SMX concentrations.

221 The retransformation of 4-nitro-SMX into SMX was confirmed by a supplementary
222 experiment in Nödler et al. (2012), which proved the reduction of 4-nitro-SMX to its
223 corresponding amino-compound (SMX) in the absence of denitrification. The molecular
224 mechanism proposed is reductive degradation, similar to the degradation of nitrobenzene to
225 aniline (Figure S2 Supplementary Material), involving an overall inclusion of 6H^+ and the
226 removal of $2\text{H}_2\text{O}$ molecules. The reductive degradation could be mediated biotically (e.g.,
227 Peres et al. 1998) or abiotically, with no information available to allow discriminating between
228 them.

229 Concerning the fate of desamino-SMX and considering the mass balance in the NDL
230 experiment, it seemed logical to infer that it was also retransformed into SMX. The most

231 common mechanism for the reintroduction of nitrogen functionality into aromatic rings (in
232 form of nitro radical) is nitration, which would imply creating a nitro-aromatic compound, here
233 again 4-nitro-SMX. After that, the nitro compound could be reduced easily to the
234 corresponding amino derivatives, as conceptualized by Carey and Sundberg 2007 and Nödler
235 et al. 2012. The active nitrating species would be the nitronium ion, NO_2^+ (Carey and Sundberg
236 2007), which would be formed by the protonation and dissociation of nitric acid in the
237 presence of sulfuric acid, acting as a catalyzer (Figure S3, Supplementary Material). As these
238 two compounds were present in the BAR and NDL experiments at similar concentrations of
239 SMX, this is a plausible mechanism.

240 To sum up, the complete conceptual model of SMX under denitrifying conditions
241 would imply the formation of two metabolites (4-nitro-SMX and desamino-SMX), which are
242 not stable and are retransformed to the parent compound, directly in the case of 4-nitro-SMX
243 or with a previous transformation to nitro compound for desamino-SMX. The full reaction
244 chain is summarized in Figure 3.

245 **2.1.3 SMX behavior under Fe reducing conditions. Observations and process inference**

246 Degradation of SMX under iron reducing conditions was described in Mohatt et al. (2011)
247 based on experimental work. The authors proposed a process based on the electron flow
248 produced by the re-oxidation of ferrous iron (II) to ferric iron (III) taking place on the surface of
249 goethite, which facilitates the break of the SMX molecule. As Fe(II) was previously produced by
250 biological reduction of Fe(III), the degradation of SMX occurred, again, as a result of a co-
251 metabolism process initiated by labile organic carbon degradation.

252 The conceptualization of this degradation process is summarized in Figure 4. The
253 metabolite formed is the result of the breakage of the isoxazole ring. Following this break, four
254 metabolites can be formed (see Table 3), each one following a particular degradation pathway
255 (Mohatt et al. 2011).

256 Note that depending on the existing redox state, the metabolites generated are very
 257 different. Whereas during denitrification the metabolites formed involve the reversible
 258 substitution of the amine radical, during either aerobic or iron reduction conditions the
 259 isoxazole ring is irreversibly broken, thus facilitating the eventual mineralization of SMX.

260 2.2 Model development

261 2.2.1 Modeling co-metabolic degradation of SMX: coupling denitrification model with SMX 262 degradation and metabolite formation

263 As indicated in the conceptual model, we postulate that the key abiotic process controlling the
 264 degradation of the SMX in the experiments was the presence of nitrous acid linked to nitrite
 265 accumulation. The first modelling step consisted in the development of a biodenitrification
 266 model capable of accounting for the transient accumulation of nitrite, and subsequently the
 267 presence of nitrous acid. The model considered a multiple-Monod expression incorporating
 268 two terms: one for the electron donor (organic carbon) and another one for the electron
 269 acceptor, as well as two reduction steps: (1) nitrate to nitrite, and (2) nitrite to dinitrogen gas
 270 (see the matrix of rates and components in Table 4 and the complete denitrification reactions
 271 in Supplementary Material). The general Monod expression for electron donor was:

$$272 \quad r = K_{\max} \frac{[ED]}{[ED] + k_{s,ED}} \frac{[EA]}{[EA] + k_{s,EA}} \frac{k_I}{[I] + k_I} [X] \quad (1)$$

273 where $[ED]$ was the concentration of the electron donor (organic carbon), $[M_{ED} L^{-3}]$. $[EA]$ that of
 274 the electron acceptor (nitrate or nitrite, $[M_{EA} L^{-3}]$), and $[X]$ the biomass concentration $[M_X L^{-3}]$.
 275 $K_{\max} [M_{Corg} M_{Corg,X}^{-1} T^{-1}]$ was the maximum consumption rate of electron donor; and $K_{s,EA}$ and $K_{s,ED}$
 276 $[ML^{-3}]$ were half-saturation constants. The rate for the other components (electron acceptor
 277 and biomass) was expression (1) times the stoichiometric coefficients, Y_b (microbial yield, for
 278 biomass and electron donor) and Q (for electron acceptor and electron donor). As the
 279 presence of nitrate limits the reduction of nitrite (Almeida et al. 1995), an inhibition factor

280 accounting for the presence of NO_3^- , $[I]$ in $[M, L^{-3}]$, was added to the electron donor rate, with
281 a constant $k_I [ML^{-3}]$.

282 The time evolution of denitrifying biomass was not measured. For simplicity, it was considered
283 constant in time, but active only after a certain elapsed time (lag phase). The actual value was
284 1 mM, consistent with available models of denitrification in batch experiments (Rodríguez-
285 Escalas et al. 2014). The lag phases were 1.8 and 3 days corresponding to the period of inactive
286 biomass for the BAR and NDL experiments, respectively. Nitrous acid concentration was
287 calculated considering its equilibrium with nitrite and a pKa of 3.15 (expression 3 at Table 4).
288 On the other hand, nitric acid concentration was assumed equal to the proton concentration
289 since this acid is strong and its concentration depends on the limiting former (protons in this
290 case).

291 The rate expressions of SMX metabolite formation were defined for each one of the
292 processes already conceptualized in Section 2.2 and Table 4. The formation of 4-nitro-SMX was
293 modelled as second-order with respect to nitrous acid (proportional to the square of the
294 concentration) and as a first-order (linear) with respect to the SMX concentration, resulting in
295 a global third-order expression. On the other hand, desamino-SMX formation was modelled as
296 a third-order kinetic expression, being first-order with respect to organic matter (methanol),
297 nitrous acid and SMX (see Table 4 for the actual expressions). The retransformation of 4-nitro-
298 SMX into SMX was modelled as a first-order degradation with respect to the metabolite. This
299 model was previously applied in a side experiment of Nödler et al. (2012), where 4-nitro-SMX
300 was converted into SMX in absence of denitrifying conditions and oxygen. Finally, the
301 retransformation of desamino-SMX into the nitro compound was considered first-order with
302 respect to the nitric acid and the metabolite, resulting in a second-order expression. The
303 election of these rates orders was the outcome of the calibration process including the
304 development of an appropriate conceptual model. Note that the order of the described
305 expressions matched to the stoichiometry of the reactions for abiotic and not catalyzed

306 reactions (see Figure S1 from Supplementary Material and Table 4). Denoting the
 307 concentrations of sulfamethoxazole, 4-nitro-SMX and desamino-SMX respectively as $[SMX]$,
 308 $[4-NIT]$, and $[DES]$, the corresponding driving equations read

$$309 \quad \frac{d[4-NIT]}{dt} = k_1[SMX][HNO_2]^2 - k_3[4-NIT] + k_4[DES][HNO_3] \quad (9)$$

$$310 \quad \frac{d[DES]}{dt} = k_2[SMX][HNO_2][C_{org}]P - k_4[DES][HNO_3]. \quad (10)$$

311 In (2) and (3) all concentrations were expressed in $[ML^{-3}]$. Additional concentrations in
 312 these equations are $[HNO_2]$, $[HNO_3]$, $[C_{org}]$, respectively standing for nitrous acid, nitric acid,
 313 and labile organic carbon. The different parameters involved are k_1, k_2 [both in $L^6 M^{-2} T^{-1}$], k_3
 314 $[T^{-1}]$, and k_4 $[L^3 M^{-1} T^{-1}]$; P is the portion of methanol in the organic matter, 0.43 in BAR and
 315 0.94 in ND. Note that the rate of SMX would be equal to the sum of (9) and (10) with a change
 316 of sign, as we assume $[SMX] + [4-NIT] + [DES] = [SMX]_0$ (that is, the initial concentration
 317 of SMX).

318 Regarding the parameters of the model, the stoichiometric ones were determined from
 319 the reactions of denitrification (Table 4 and Section 2 of Supplementary Material). The kinetic
 320 parameters (K_{max}, k_s, k_i for the denitrification model, and k_1, k_2, k_3, k_4 for the SMX degradation
 321 model) were automatically calibrated using code PEST (Doherty 2005). Notice that this process
 322 involved two independent (not simultaneous) calibration processes. PEST code allowed
 323 computing the sensitivities, correlations, and linear uncertainties (confidence intervals) for the
 324 optimized model parameters using the Levenberg-Marquardt algorithm. The weights of each
 325 chemical species (ω_i) associated to the measurement errors (ε_i) were applied using the
 326 inverse of the standard deviation of the confidence interval of measurements (95%). For the
 327 calibration process, we used the experimental information (nitrate, nitrite, SMX, 4-nitro-SMX
 328 and desamino-SMX) provided by Barbieri et al. (2012) and Nödler et al. (2012). The initial
 329 concentrations of the model are summarized in Table 2. Note that the initial concentration of

330 SMX in the model of NDL experiment represented 45% of the initial one (1.8 μM). This was
331 because the concentration of SMX suddenly decreased during the lag phase (Figure 2).
332 Afterwards the mass balance remained constant.

333 **2.2.2 Mathematical model and application to the interpretation of experiments of SMX** 334 **under iron reducing conditions**

335 The original model of SMX degradation under iron reducing conditions proposed by Mohatt et
336 al. (2011) assumes an exponential decay for SMX, focusing on a single abiotic degradation
337 process. Our conceptual model is based on the reaction occurring on the surface of goethite,
338 having a significantly different behavior at early times and at late times. At early times the
339 exponential model fits properly the experimental data of Mohatt et al. (2011); this implies that
340 the model is based on a large number of available sites for reaction at the goethite surface.
341 Once these sites are mostly exhausted (intermediate to large times), additional ones must be
342 found at deeper layers. The number of sites at those deep layers can be best modeled using a
343 fractal approach, so that the reaction rate is best described by a power law. Thus, the
344 governing equations are:

$$345 \quad \frac{d[\text{SMX}]}{dt} = \begin{cases} -k_5[\text{SMX}] \\ -k_6[\text{SMX}]^n \end{cases} \quad (11)$$

346 where k_5 [T^{-1}] and k_6 [$\text{M}^{1-n}\text{L}^{3n-3}\text{T}^{-1}$] are degradation constants. The top expression in (11) is
347 applicable for short times and the bottom one would be valid for intermediate to large times,
348 with a transition of behavior not clearly defined.

349

350 **3 Results and discussion**

351 **3.1 Fate of SMX and metabolites under denitrifying and iron reducing conditions**

352 Figure 2 displays the results of the modelling effort applied to the BAR (top row) and NDL
353 (bottom) using the best-fitted parameters listed in Table 5. Figures 2a and 2d correspond to

354 the biodenitrification process in terms of nitrate and nitrite concentrations. The corresponding
355 inferred (not measured) presence of nitrous acid is displayed in Figures 2b and 2e. These same
356 plots present the model fit of the concentrations of SMX and the two metabolites (only one in
357 the BAR experiment). SMX concentrations are reasonably well reproduced with the only
358 exception of the last point in the BAR experiment; we associate this misfit to the model not
359 accounting for iron/manganese reduction conditions developing after 10 days. Regarding the
360 concentration of 4-nitro-SMX, the model reproduced quantitatively the temporal behavior in
361 both experiments. In addition desamino-SMX concentrations were well reproduced for the
362 NDL experiment (in the BAR experiment, Figure 2b, this value was only inferred, and plotted as
363 a green dashed line).

364 The results of the calibration of the SMX degradation model are displayed in Table 5. The
365 parameters inferred display a high degree of uncertainty, being larger in the BAR experiment.
366 This is probably due to the lack of measurements regarding one of the metabolites (desamino-
367 SMX), affecting the values of k_2 , k_4 through equation (2), with such uncertainty propagating
368 to k_1 and k_3 . Furthermore, the correlation matrix displayed by PEST showed that there was
369 no correlation among the parameters (all values were lower than 0.55, results not shown).

370 Note that despite modeling the same processes in the two experiments, the parameters
371 determined in BAR and NDL are quite different being higher in the former (for example k_1 and
372 k_2 are two orders of magnitude higher). All but first-order degradation rates (third-order in the
373 nitrosation of the primary amines and second-order in the nitration of the benzene ring) are
374 dependent on initial conditions (Atkins and de Paula 2011). As the initial conditions were three
375 orders of magnitude different, it is evident that the parameters were not able to be compared.
376 Furthermore, the high concentration of SMX in NDL experiment could represent some type of
377 biomass inhibition and could be another reason for such differences. Nevertheless, we did not
378 have enough experimental data to characterize if this existed and if it had any consequence.

379 Regarding the degradation of SMX under iron-reducing conditions, the best fit was
380 obtained using the automatically calibrated by PEST parameters (see section 3.1.1) and they
381 are listed in Table 5, and the actual fit to data is displayed in Figure 5. Actually, in the same
382 Figure the fit with an exponential model is also presented, here focused only on early time
383 data, to show the transition in behavior as a function of time. Note that all potential
384 degradation pathways described would be naturally limited by the low amount of organic
385 carbon in the subsoil. Besides this, iron-reducing conditions will only be reached when all the
386 previous redox states were ended. Thus, the amount of organic carbon supplied to the system
387 is key. Once iron reducing conditions were achieved, the degradation of SMX is achieved in
388 hours (Figure 5).

389 **3.2 Potential extensions to real field site applications**

390 The main reactive path for the degradation of SMX under denitrifying conditions involves the
391 presence of nitrous acid that accumulates associated with the building up (and further decay)
392 of nitrite. Nitrite is a usual transient compound in denitrification processes. Its accumulation
393 can be, traditionally, explained by different reasons: 1) the presence of low levels of oxygen
394 (up to 0.7 mg/l) (Coyne and Tiedje 1990); 2) the competition between nitrate and nitrite
395 enzymes for a common electron donor (Thomsen et al. 1990); 3) large differences in the
396 maximum reduction rates of nitrate and nitrite reductases (Betlach and Tiedje 1981); and 4)
397 the choice of carbon source (van Rijn et al. 1996). In addition, the presence of antibiotics is
398 suggested to inhibit the reduction step from nitrate to nitrite (Yan et al. 2013), and thus
399 facilitate nitrite accumulation and nitrous acid formation. Other studies also suggested that a
400 continuous exposition to SMX in large quantities will affect the bacterial denitrifying
401 community (Underwood et al. 2011). Consequently, the presence of 4-nitro-SMX would be
402 quite plausible in natural aqueous environments where nitrate and antibiotics leakage
403 converge, such as rural areas where nitrate and veterinarian antibiotics coexist (García-Galán
404 et al. 2010). As the formation of desamino-SMX will be conditioned to the presence of alcohol

405 which is not always present in organic matter, we expect that in real site applications 4-nitro-
406 SMX will be the dominant metabolite. If we consider that alcohol and, therefore, desamino-
407 SMX are not present, we could assume that SMX would only transition to 4-nitro-SMX.

408 There is an increasing concern in the possibility that metabolites produced during the
409 degradation of emerging compounds will be more hazardous to either human health or
410 ecosystem than the parent itself. For that, we compared the LC₅₀ for *Daphnia sp.* (after 48 h)
411 and fish (after 96 h) calculated by ECOSAR packet of EPI-SUITE (USEPA 2012), for all
412 metabolites evaluated in this work (Table 6). Both *Daphnia sp.* and fish were used as proxies of
413 the full ecosystem. In Table 6 we have also included partition coefficients as well as solubility
414 for each compound in order to compare the impact to the environment. Although the
415 presented concentrations of toxicity are referred to the acute toxicity and they are much
416 higher than the environmental concentrations of SMX, they serve as a comparative criterion.
417 Overall, 4-nitro-SMX was the most toxic compound (lowest LC₅₀). The toxicity was associated
418 to the nitroaromatic compounds which are acutely toxic and mutagenic, and many are
419 suspected or established carcinogens (Ju and Parales 2010). On the other hand, metabolites
420 conserving the isoxazole ring (Product II in Table 3 and 3-amino-5-methylisoxazole) are more
421 toxic when compared to SMX. Contrarily, 4-aminobenzosulfonate and metabolites produced
422 under iron reducing conditions with broken isoxazole ring (Products III and IV in Table 3) are
423 the least toxic of all the compounds studied, and probably they can be mineralized easily (Gao
424 et al. 2010). These results are perfectly correlated with values of logK_{ow} and solubility. The
425 highest values of logK_{ow} correlated to the highest value of LC₅₀, and at the same time, the
426 highest values of solubility correspond to low risk compounds. High solubility and low values of
427 K_{ow} indicate that all the metabolites will remain mainly in water, with low absorptivity rates
428 into solid phases.

429 From the combination of reversibility and environmental fate/risk, it seems reasonable
430 to conclude that the most efficient degradation path to remove all presence of SMX from

431 groundwater bodies involves allowing the aquifer to reach iron reducing conditions. We want
432 to stress here that this conclusion is only valid for SMX, and thus a potential intelligent
433 methodology to eliminate a cocktail of emerging organic compound and their metabolites
434 would be to allow the aquifer to reach many different redox states, each one of them being
435 the most efficient one for the degradation of a given molecule. At this point there is a need in
436 the future to investigate many more molecules and even the synergic effect of injecting
437 several compounds together.

438 In any case, and indistinctly to the redox process, the degradation of SMX is driven by
439 co-metabolism enhanced by the presence of external labile organic carbon. In this way, it
440 might be possible to properly manage the amount of labile organic carbon in the system, thus
441 properly allowing the control (in space and time) of redox zonation for the proper
442 management of EOCs degradation in the subsurface. One real example of this application is
443 the installation of a labile organic carbon layer (compost) on the bottom of an infiltration pond
444 in a managed aquifer recharge facility that enhanced EOCs degradation (Schaffer et al. 2015,
445 Valhondo et al. 2014, Valhondo et al. 2015). The induced redox zonation by the oxidation of
446 labile organic carbon increased the possibilities of degradation of different emerging
447 compounds, here including sulfamethoxazole.

448

449 **4 Conclusions**

450 In this work we have conceptualized and modelled the degradation path of the SMX
451 (sulfamethoxazole) molecule under different redox conditions in groundwater. We have
452 developed a model capable of reproducing the fate of SMX as well as its metabolites under
453 different redox conditions. Our model is based on the understanding of the real molecular
454 mechanism of degradation instead of using simplified models postulating first-order
455 degradation models, based on the apparent degradation behavior of SMX in experiments.

456 Our model focused on denitrifying and iron-reducing conditions, being the dominant
457 ones for SMX degradation in groundwater. The main reactive path for the degradation of SMX
458 under denitrification involves the presence of nitrous acid, which promotes the nitrosation of
459 the primary amine of SMX forming 4-nitro-SMX. If alcohol is present in the system a second
460 metabolite is produced, desamino-SMX. Both of them are unstable and can eventually be
461 retransformed to the parent compound. Biologically iron reduction conditions would facilitate
462 the break of the SMX molecule through enhancing the abiotic mechanism of oxidation of
463 ferrous iron to ferric iron. Several metabolites may be formed, involving the break of the
464 isoxazole ring in the SMX molecule and individual potential degradation pathways.

465 The mathematical model proposed for SMX degradation under denitrifying conditions
466 involves different forward and backward processes with complex kinetic rates. For 4-nitro-SMX
467 two forward processes arise, one involving SMX and the concentration of HNO_2 squared, and a
468 second one proportional to the concentration of desamino-SMX and also to that of HNO_3 . The
469 backward term implies linear first-order degradation. For desamino-SMX there is one forward
470 term, proportional to the concentrations of SMX, HNO_2 and organic carbon in the form of
471 alcohol, and a backward one proportional to the concentrations of desamino-SMX and HNO_3 .

472 The model presented is capable of properly reproducing the results from two
473 experiments reported in the literature. The actual parameters present in the governing
474 equations are strongly influenced by the initial concentration of the SMX. In the case of iron
475 reducing conditions it was found that the best reproduction of a batch experiment is obtained
476 by a combination of an exponential model at short times and a power law function at large
477 times.

478 The shortest reported characteristic time for degradation of the SMX molecule
479 corresponds to iron reducing conditions. Also, in this case, it was found that the metabolites
480 produced under iron reducing conditions are the most convenient in terms of minimizing total
481 risk to ecosystems. The work performed in SMX could be extended to other EOCs, and each

482 one of them is expected to behave differently and to be best degraded for some specific redox
483 conditions. Thus, in real field applications the optimal combination to degrade a suite of EOCs
484 would be to enhance redox zonation by an engineered introduction of organic carbon in the
485 aquifer.

486 **5 Acknowledgements**

487 We thank the three reviewers and the associate editor for their comments and suggestions,
488 which helped improve the quality of the manuscript. Financial support was provided by the
489 European Union, project MARSOL FP7-ENV-2013-WATER-INNO-DEMO and by Spanish
490 government, project INDEMNE, CGL2015-69768-R. XSV acknowledges support by the ICREA
491 Academia Program.

492 **6 References**

- 493 Almeida, J.S., Reis, M.A. and Carrondo, M.J. (1995) Competition between nitrate and nitrite
494 reduction in denitrification by *Pseudomonas fluorescens*. Biotechnol. Bioeng. 46(5), 476-
495 484.
- 496 Atkins, P. and de Paula, J. (2011) Physical Chemistry for the life sciences. Second edition.
- 497 Banzhaf, S., Nödler, K., Licha, T., Krein, A. and Scheytt, T. (2012) Redox-sensitivity and mobility
498 of selected pharmaceutical compounds in a low flow column experiment. Sci. Total Environ.
499 438(0), 113-121.
- 500 Barbieri, M., Carrera, J., Ayora, C., Sanchez-Vila, X., Licha, T., Nodler, K., Osorio, V., Perez, S.,
501 Kock-Schulmeyer, M., Lopez de Alda, M. and Barcelo, D. (2012) Formation of diclofenac and
502 sulfamethoxazole reversible transformation products in aquifer material under denitrifying
503 conditions: batch experiments. Sci. Total Environ. 426, 256-263.
- 504 Barbieri, M., Carrera, J., Sanchez-Vila, X., Ayora, C., Cama, J., Köck-Schulmeyer, M., López de
505 Alda, M., Barceló, D., Tobella Brunet, J. and Hernández García, M. (2011) Microcosm

506 experiments to control anaerobic redox conditions when studying the fate of organic
507 micropollutants in aquifer material. *J. Contam. Hydrol.* 126(3–4), 330-345.

508 Baumgarten, B., Jährig, J., Reemtsma, T. and Jekel, M. (2011) Long term laboratory column
509 experiments to simulate bank filtration: Factors controlling removal of sulfamethoxazole.
510 *Water Res.* 45(1), 211-220.

511 Betlach, M.R. and Tiedje, J.M. (1981) Kinetic explanation for accumulation of nitrite, nitric
512 oxide, and nitrous oxide during bacterial denitrification. *Applied and Environmental*
513 *Microbiology* 42(6), 10.

514 Carey, F.A. and Sundberg, R.J. (2007) *Advanced Organic Chemistry. Part B: Reactions and*
515 *Synthesis.*, Springer.

516 Coyne, M.S. and Tiedje, J.M. (1990) Induction of denitrifying enzymes in oxygen-limited
517 *Achromobacter cycloclastes* continuous culture. *FEMS Microbiology Letters* 73(3), 263-270.

518 Doherty, J. (2005) PEST: model independent parameter estimation. *Watermark Numerical*
519 *Computing*, fifth edition of user manual.

520 Drillia, P., Dokianakis, S.N., Fountoulakis, M.S., Kornaros, M., Stamatelatou, K. and Lyberatos,
521 G. (2005) On the occasional biodegradation of pharmaceuticals in the activated sludge
522 process: The example of the antibiotic sulfamethoxazole. *Journal of Hazardous Materials*
523 122(3), 259-265.

524 Everett, M. (1973) Deamination by the diazotization-deazotization method. *Histochem. J.* 5(1),
525 1-7.

526 Fent, K., Weston, A.A. and Caminada, D. (2006) Ecotoxicology of human pharmaceuticals.
527 *Aquat. Toxicol.* 76(2), 122-159.

528 Gao, J., Ellis, L.B.M. and Wackett, L.P. (2010) The University of Minnesota
529 Biocatalysis/Biodegradation Database: improving public access. *Nucleic Acid Res* 38(suppl
530 1), D488-D491.

531 Gao, S., Zhao, Z., Xu, Y., Tian, J., Qi, H., Lin, W. and Cui, F. (2014) Oxidation of sulfamethoxazole
532 (SMX) by chlorine, ozone and permanganate—A comparative study. *J. Hazard. Mat.* 274(0),
533 258-269.

534 García-Galán, M.J., Garrido, T., Fraile, J., Ginebreda, A., Díaz-Cruz, M.S. and Barceló, D. (2010)
535 Simultaneous occurrence of nitrates and sulfonamide antibiotics in two ground water
536 bodies of Catalonia (Spain). *J. Hydrol.* 383(1–2), 93-101.

537 Gauthier, H., Yargeau, V. and Cooper, D.G. (2010) Biodegradation of pharmaceuticals by
538 *Rhodococcus rhodochrous* and *Aspergillus niger* by co-metabolism. *Science of The Total*
539 *Environment* 408(7), 1701-1706.

540 Gavrilesco, M., Demnerová, K., Aamand, J., Agathos, S. and Fava, F. (2015) Emerging pollutants
541 in the environment: present and future challenges in biomonitoring, ecological risks and
542 bioremediation. *New Biotechnol.* 32(1), 147-156.

543 Greskowiak, J., Prommer, H., Massmann, G. and Nützmann, G. (2006) Modeling Seasonal
544 Redox Dynamics and the Corresponding Fate of the Pharmaceutical Residue Phenazone
545 During Artificial Recharge of Groundwater. *Environ. Sci. Technol.* 40(21), 6615-6621.

546 Grünheid, S., Amy, G. and Jekel, M. (2005) Removal of bulk dissolved organic carbon (DOC) and
547 trace organic compounds by bank filtration and artificial recharge. *Water Res.* 39(14), 3219-
548 3228.

549 Göbel, A., Thomsen, A., McArdell, C.S., Joss, A. and Giger, W. (2005) Occurrence and Sorption
550 Behavior of Sulfonamides, Macrolides, and Trimethoprim in Activated Sludge Treatment.
551 *Environ. Sci. Technol.* 39(11), 3981-3989.

552 Heberer, T. (2002) Occurrence, fate, and removal of pharmaceutical residues in the aquatic
553 environment: a review of recent research data. *Toxicol. Lett.* 131(1–2), 5-17.

554 Heberer, T., Massmann, G., Fanck, B., Taute, T. and Dünnebier, U. (2008) Behaviour and redox
555 sensitivity of antimicrobial residues during bank filtration. *Chemosphere* 73(4), 451-460.

556 Henzler, A.F., Greskowiak, J. and Massmann, G. (2014) Modeling the fate of organic
557 micropollutants during river bank filtration (Berlin, Germany). *J. Contam. Hydrol.* 156(0), 78-
558 92.

559 Hirsch, R., Ternes, T., Haberer, K. and Kratz, K.-L. (1999) Occurrence of antibiotics in the aquatic
560 environment. *Sci. Total Environ.* 225(1–2), 109-118.

561 Ji, Y., Ferronato, C., Salvador, A., Yang, X. and Chovelon, J.M. (2014) Degradation of
562 ciprofloxacin and sulfamethoxazole by ferrous-activated persulfate: implications for
563 remediation of groundwater contaminated by antibiotics. *Sci. Total Environ.* 472, 800-808.

564 Jjemba, P.K. (2002) The potential impact of veterinary and human therapeutic agents in
565 manure and biosolids on plants grown on arable land: a review. *Agr. Ecosyst. Environ.* 93(1–
566 3), 267-278.

567 Ju, K.-S. and Parales, R.E. (2010) Nitroaromatic Compounds, from Synthesis to Biodegradation.
568 *Microbiol Mol Biol Rev.* 74(2), 250-272.

569 Liu, Y.-S., Ying, G.-G., Shareef, A. and Kookana, R.S. (2013) Biodegradation of three selected
570 benzotriazoles in aquifer materials under aerobic and anaerobic conditions. *J. Contam.*
571 *Hydrol.* 151, 131-139.

572 Mohatt, J.L., Hu, L., Finneran, K.T. and Strathmann, T.J. (2011) Microbially mediated abiotic
573 transformation of the antimicrobial agent sulfamethoxazole under iron-reducing soil
574 conditions. *Environ. Sci. Technol.* 45(11), 4793-4801.

575 Morrisson, R.T. and Boyd, R.N. (1992) *Organic Chemistry*, 6th edition, Prentice-Hall, Inc. A
576 Paramount Communications Company.

577 Müller, E., Schüssler, W., Horn, H. and Lemmer, H. (2013) Aerobic biodegradation of the
578 sulfonamide antibiotic sulfamethoxazole by activated sludge applied as co-substrate and
579 sole carbon and nitrogen source. *Chemosphere* 92(8), 969-978.

580 Nham, H.T.T., Greskowiak, J., Nödler, K., Rahman, M.A., Spachos, T., Rusteberg, B., Massmann,
581 G., Sauter, M. and Licha, T. (2015) Modeling the transport behavior of 16 emerging organic
582 contaminants during soil aquifer treatment. *Sci. Total Environ.* 514(0), 450-458.

583 Nödler, K., Licha, T., Barbieri, M. and Pérez, S. (2012) Evidence for the microbially mediated
584 abiotic formation of reversible and non-reversible sulfamethoxazole transformation
585 products during denitrification. *Water Res.* 46(7), 2131-2139.

586 Peres, C.M., Naveau, H. and Agathos, S.N. (1998) Biodegradation of nitrobenzene by its
587 simultaneous reduction into aniline and mineralization of the aniline formed. *Appl.*
588 *Microbiol. Biotechnol.* 49(3), 343-349.

589 Reis, P.J.M., Reis, A.C., Ricken, B., Kolvenbach, B.A., Manaia, C.M., Corvini, P.F.X. and Nunes,
590 O.C. (2014) Biodegradation of sulfamethoxazole and other sulfonamides by *Achromobacter*
591 *denitrificans* PR1. *J. Hazard. Mat.* 280(0), 741-749.

592 Rodríguez-Escales, P., van Breukelen, B., Vidal-Gavilan, G., Soler, A. and Folch, A. (2014)
593 Integrated modeling of biogeochemical reactions and associated isotope fractionations at
594 batch scale: A tool to monitor enhanced biodenitrification applications. *Chem. Geol.* 365(0),
595 20-29.

596 Schaffer, M., Kröger, K.F., Nödler, K., Ayora, C., Carrera, J., Hernández, M. and Licha, T. (2015)
597 Influence of a compost layer on the attenuation of 28 selected organic micropollutants
598 under realistic soil aquifer treatment conditions: Insights from a large scale column
599 experiment. *Water Res.* 74(0), 110-121.

600 Schwarzenbach, R.P., Escher, B.I., Fenner, K., Hofstetter, T.B., Johnson, C.A., von Gunten, U.
601 and Wehrli, B. (2006) The Challenge of Micropollutants in Aquatic Systems. *Science*
602 313(5790), 1072-1077.

603 Stadler, L.B., Su, L., Moline, C.J., Ernstoff, A.S., Aga, D.S. and Love, N.G. (2015) Effect of redox
604 conditions on pharmaceutical loss during biological wastewater treatment using sequencing
605 batch reactors. *J. Hazard. Mater.* 282, 106-115.

606 Szczepanowski, R., Linke, B., Krahn, I., Gartemann, K.H., Gutzkow, T., Eichler, W., Puhler, A. and
607 Schluter, A. (2009) Detection of 140 clinically relevant antibiotic-resistance genes in the
608 plasmid metagenome of wastewater treatment plant bacteria showing reduced
609 susceptibility to selected antibiotics. *Microbiology* 155(Pt 7), 2306-2319.

610 Thomsen, J.K., Geset, T. and Cox, R.P. (1990) Mass spectrometric studies of the effect of pH on
611 the accumulation of intermediates in denitrification by *Paracoccus denitrificans*. *Applied*
612 *Environmental Microbiology* 60(2), 5.

613 Underwood, J.C., Harvey, R.W., Metge, D.W., Repert, D.A., Baumgartner, L.K., Smith, R.L.,
614 Roane, T.M. and Barber, L.B. (2011) Effects of the Antimicrobial Sulfamethoxazole on
615 Groundwater Bacterial Enrichment. *Environ. Sci. Technol.* 45(7), 3096-3101.

616 USEPA (2012) Estimation Programs Interface Suite™ for Microsoft® Windows.

617 Valhondo, C., Carrera, J., Ayora, C., Barbieri, M., Nodler, K., Licha, T. and Huerta, M. (2014)
618 Behavior of nine selected emerging trace organic contaminants in an artificial recharge
619 system supplemented with a reactive barrier. *Environ. Sci. Pollut. Res. Int.* 21(20), 11832-
620 11843.

621 Valhondo, C., Carrera, J., Ayora, C., Tubau, I., Martinez-Landa, L., Nödler, K. and Licha, T. (2015)
622 Characterizing redox conditions and monitoring attenuation of selected pharmaceuticals
623 during artificial recharge through a reactive layer. *Sci. Tot. Environ.* 512–513(0), 240-250.

624 van Rijn, J., Tal, Y. and Barak, Y. (1996) Influence of Volatile Fatty Acids on Nitrite Accumulation
625 by a *Pseudomonas*. *Appl. Environ. Microbiol.* 62(7), 2615-2620.

626 Yan, C., Dinh, Q.T., Chevreuril, M., Garnier, J., Roose-Amsaleg, C., Labadie, P. and Laverman,
627 A.M. (2013) The effect of environmental and therapeutic concentrations of antibiotics on
628 nitrate reduction rates in river sediment. *Water Res.* 47(11), 3654-3662.

629

630 **Figure captions**

631 **Figure 1.** Pathway of aerobic degradation of SMX proposed by Gao et al. (2010) and later
632 confirmed experimentally by Müller et al. (2013) and Reis et al. (2014).

633 **Figure 2.** Experimental information of Barbieri et al. (2012) (a, b, c) and Nödler et al. (2012) (d,
634 e, f) (points) and modelled results of nitrate and nitrite (a,d), sulfamethoxazole, 4-nitro
635 sulfamethoxazole, desamino-sulfamethoxazole and nitrous acid (b,d). The time axis is
636 displayed in log scale. The extremes of the bars associated with each individual measurement
637 indicate the values obtained from two replicates, while dots display their arithmetic average.
638 Solid lines represent the results from the modeling effort (Section 3.1). Dashed lines in b) and
639 e) represent expected (from the model) concentrations of non-measured elements.

640 **Figure 3.** Conceptual model of processes involved in the fate of SMX under denitrifying
641 conditions (*italic letters*) and the corresponding metabolites.

642 **Figure 4.** Conceptual model of SMX due to the abiotic oxidation of iron due to a previous
643 reduction of goethite biologically mediated (modified from Mohatt et al. (2011)).

644 **Figure5.** Experimental point (from Mohatt et al. (2011)) and modelling results using first-order
645 degradation rate and power law.

646

647 **Table caption**

648 **Table 1.** Compilation of values of degradation half-time reported in the literature for aerobic
649 degradation of SMX assuming first-order reaction.

650 **Table 2.** Main compounds in the input water used in the BAR and NDL experiments. The
651 complete hydrochemistry can be consulted in Barbieri et al. (2012) and Nödler et al. (2012).

652 **Table 3.** Metabolites of SMX detected during iron reducing conditions (modified from Mohatt
653 et al. 2011).

654 **Table 4.** Processes, components and rates involved during degradation of SMX under
655 denitrifying conditions. The stoichiometric coefficients were determined from complete
656 reactions (Section 2 for denitrification and Fig. S1 and S2 for SMX under denitrifying
657 conditions).

658 **Table 5.** Model parameters (mean and standard deviation, SD) used in denitrification model
659 and SMX degradation models.

660 **Table 6.** Octanol partition coefficient, solubility and LC_{50} of SMX and all metabolites evaluated
661 in this work. All these values were estimated using ECOSAR package of EPI-SUITE (USEPA
662 2012).

Table1

[Click here to download Table: SMX_table1_v3.docx](#)

Work	$T_{1/2}$ ($T_{1/2}=\ln 2/k$)	Experimental conditions
Baumgarten et al., 2011	1 - 9 d (calculated with biomass acclimated during 28 weeks of experiment)	Column experiment Aerobic surface water Concentrations of SMX were between 0.25 and 4.15 $\mu\text{g/L}$
Gauthier et al., 2010	35 d	Batch experiment (<i>R. rhodocrous</i>) Activated sludge with acclimated biomass Concentration of SMX was 31.6 mg/L
Reis et al., 2014	31, 34 and 99 d	Batch experiment Activated sludge with acclimated biomass Concentrations of SMX were between 152 and 2500 mg/L
Drillia et al., 2005	3.5 d (with acetate and nitrogen source), 10.5 d (without)	Batch experiment Concentration of SMX was 200 mg/L Activated sludge with acclimated biomass

Table2[Click here to download Table: SMX_table2_v3.docx](#)

	Barbieri experiment (BAR)	Nödler experiment (NDL)
SMX (μM)	0.004	4
Nitrate (mM)	6.7	67.7
Organic carbon (mM)	9.7	71.5
Iron (Fe^{+3}) (mM)	0.001	0.001
Manganese (Mn^{+4}) (mM)	0.001	0.001
pH	8.5	7.3
Temperature ($^{\circ}\text{C}$)	25	25

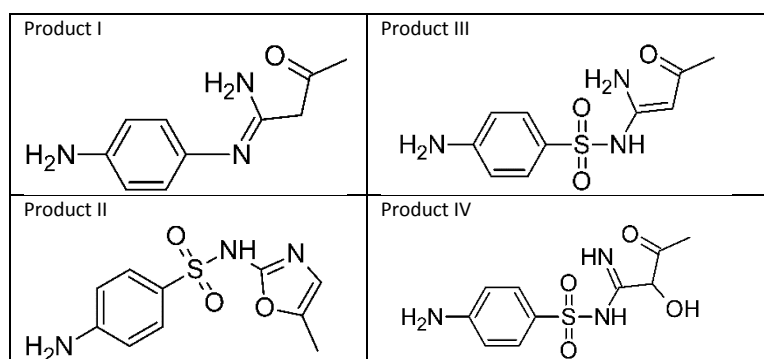
Table3[Click here to download Table: SMX_table3_v3.docx](#)

Table4
[Click here to download Table: SMX_table4_v3.docx](#)

Process	Components											Process rate
	C _{org}	C _{inorg}	NO ₃ ⁻	NO ₂ ⁻	N ₂	H ⁺	HNO ₂	HNO ₃	SMX	4-NIT	DESA M	
Organic matter degradation due to nitrate reduction	-1	+1	-2.2	+2.2								$K_{max} \frac{[C_{org}]}{[C_{org}] + k_{s,C_{org}}} \frac{[NO_3^-]}{[NO_3^-] + k_{s,NO_3^-}} [X]$ (2)
Organic matter degradation due to nitrite reduction	-1	+1		-1.5	+0.75	+1.5						$K_{max} \frac{[C_{org}]}{[C_{org}] + k_{s,C_{org}}} \frac{[NO_2^-]}{[NO_2^-] + k_{s,NO_2^-}} \frac{k_I}{[NO_3^-] + k_I} [X]$ (3)
Nitrite equilibrium with nitrous acid				-1		-1	+1					$\frac{[NO_2^-][H^+]}{K_a}$ (4)
Nitrosation of primary amine and formation of 4-nitro-SMX							-2		-1	+1		$k_1 [SMX][HNO_2]^2$ (5)
Nitrosation of primary amine and formation of desamino-SMX	-1						-1		-1		+1	$k_2 [SMX][HNO_2][C_{org}]^P$ (6)
Reduction of 4-nitro-SMX and formation of SMX									+1	-1		$k_3 [4-NIT]$ (7)
Nitration of benzene ring of desamino-SMX and formation of 4-nitro-SMX								-1		+1	-1	$k_4 [DES][HNO_3]$ (8)

Table5

[Click here to download Table: SMX_table5_v3.docx](#)

	Organic matter oxidation due to denitrification processes							
	Reduction of nitrate to nitrite		Reduction of nitrite to dinitrogen gas		Reduction of nitrate to nitrite		Reduction of nitrite to dinitrogen gas	
	Barbieri experiment				Nödler experiment			
	Mean	SD	Mean	SD	Mean	SD	Mean	SD
K_{max} (molC _{org} /mol C _x d)	19.0	3.6	11	1.1	2.0	0.8	2.0	0.5
k_{s,NO_3^-} (M)	1.0×10^{-4}	5.6×10^{-5}	-	-	3.0×10^{-3}	8.3×10^{-4}	-	-
k_{s,NO_2^-} K _{s,NO2} (M)	-	-	5.0×10^{-4}	4.8×10^{-4}	-	-	7.5×10^{-4}	5×10^{-4}
$k_{s,C_{org}}$ K _{s Corg'} (M)	1.6×10^{-1}	3.9×10^{-2}	1.8×10^{-2}	1.0×10^{-2}	1.0×10^{-1}	1.1×10^{-2}	4.3×10^{-2}	1.4×10^{-2}
k_i (M)	-	-	5×10^{-4}	7×10^{-5}	-	-	3.5×10^{-1}	3.0×10^{-1}
	Abiotic degradation of SMX enhanced by co-metabolism (denitrification)							
	Barbieri experiment				Nödler experiment			
	Mean		SD		Mean		SD	
k_1 (1/M ² d)	6.0×10^{14}		2.6×10^{15}		2.0×10^{12}		9.97×10^{11}	
k_2 (1/M ² d)	1.3×10^{10}		6.8×10^9		8.8×10^7		7.5×10^6	
k_3 (1/d)	4.93		2.88		0.39		0.108	
k_4 (1/M d)	9.2×10^6		3.8×10^5		2.1×10^6		4.11×10^5	
	Abiotic degradation of SMX enhanced by co-metabolism (iron reducing conditions)							
	k_5 (1/d)	2.7						
	k_6 (1/d)	0.96						
	n	0.91						

Table6

[Click here to download Table: SMX_table6_v3.docx](#)

	Conditions	logK _{ow}	Solubility (mg/L, 25°C)	LC ₅₀ <i>Daphnia</i> sp.	LC ₅₀ fish
Sulfamethoxazole		0.89	6.1x10 ²	2.36x10 ²	4.78x10 ³
4-amino benzosulfonate	Aerobic	-2.16	5.7x10 ²	2.57x10 ⁵	6.59x10 ⁵
3-amino-5-methyl-isoxazole	Aerobic	0.22	1.67x10 ⁵	1.09x10 ³	2.28x10 ³
4-nitro-sulfamethoxazole	Denitrifying	1.22	5.67x10 ²	6.18x10 ²	1.17x10 ³
Desamino-sulfamethoxazole	Denitrifying	1.40	1.75x10 ³	3.63x10 ²	6.75x10 ²
Product I	Iron reducing	0.19	3.35 x 10 ⁵	3.15x10 ³	6.55x10 ³
Product II	Iron reducing	0.48	8.76 x 10 ³	2.36x10 ³	4.78x10 ³
Product III	Iron reducing	-2.00	1 x 10 ⁶	3.21x10 ⁵	8.18x10 ⁵
Product IV	Iron reducing	-4.17	1 x 10 ⁶	2.5x10 ⁷	7.8x10 ⁷

Figure 1

[Click here to download high resolution image](#)

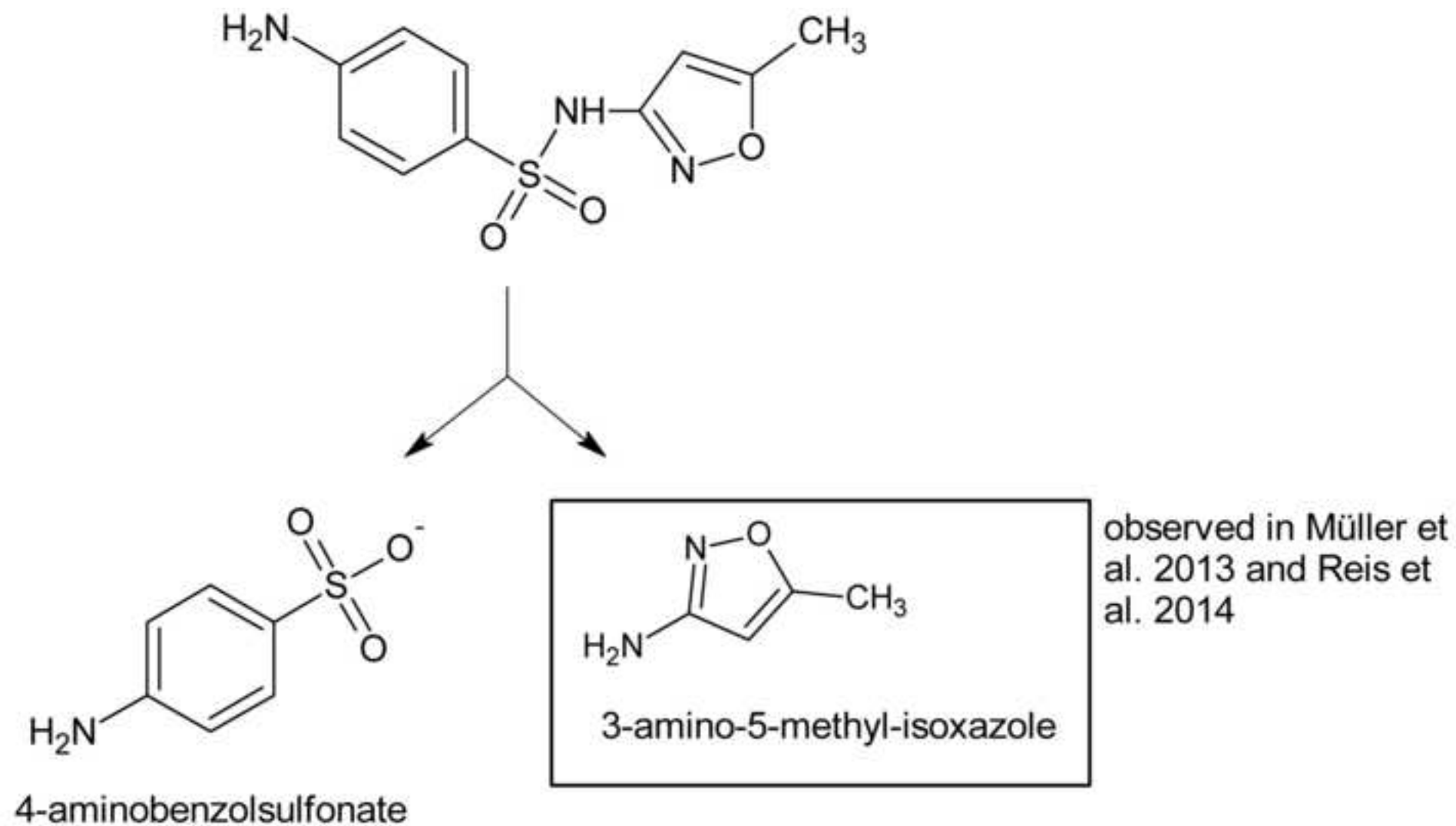


Figure2

[Click here to download high resolution image](#)

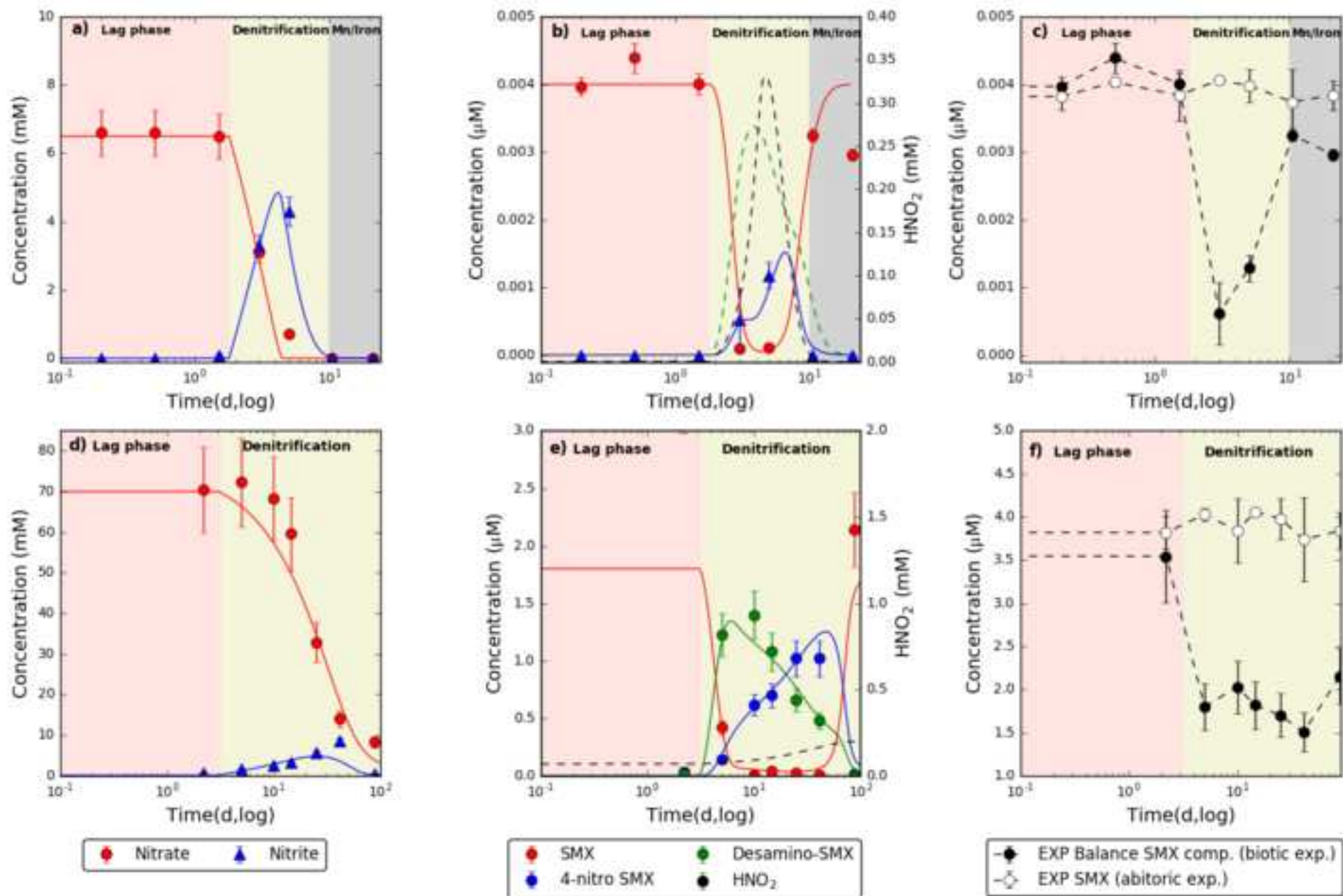


Figure3

[Click here to download high resolution image](#)

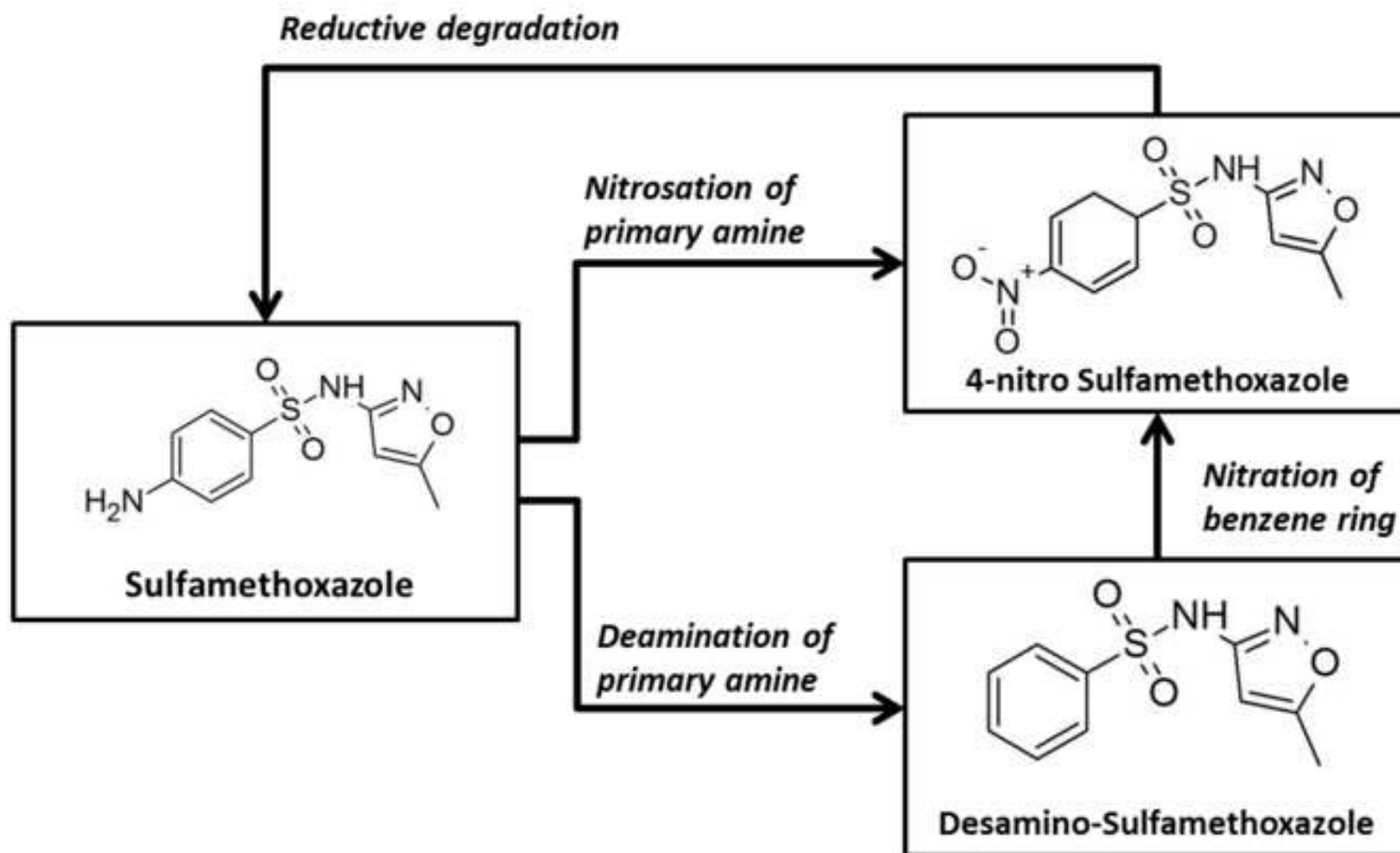


Figure4

[Click here to download high resolution image](#)

ABIOTIC DEGRADATION OF SMX DUE TO SURFACE OXIDATION OF IRON

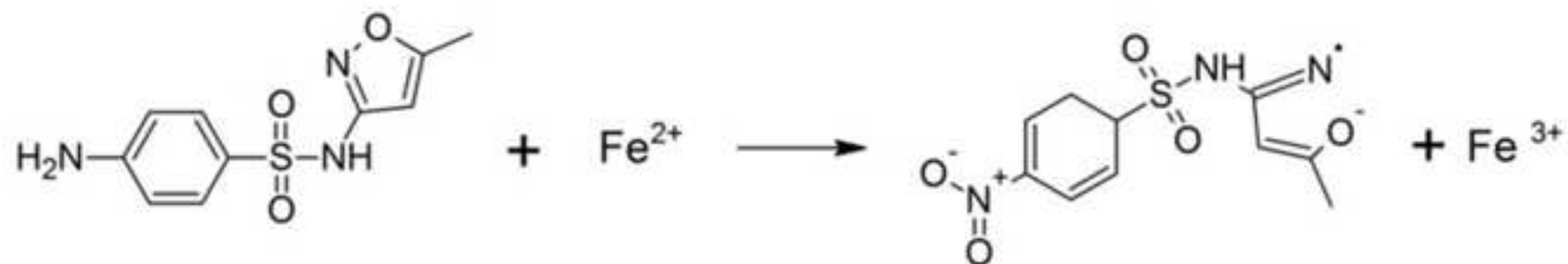
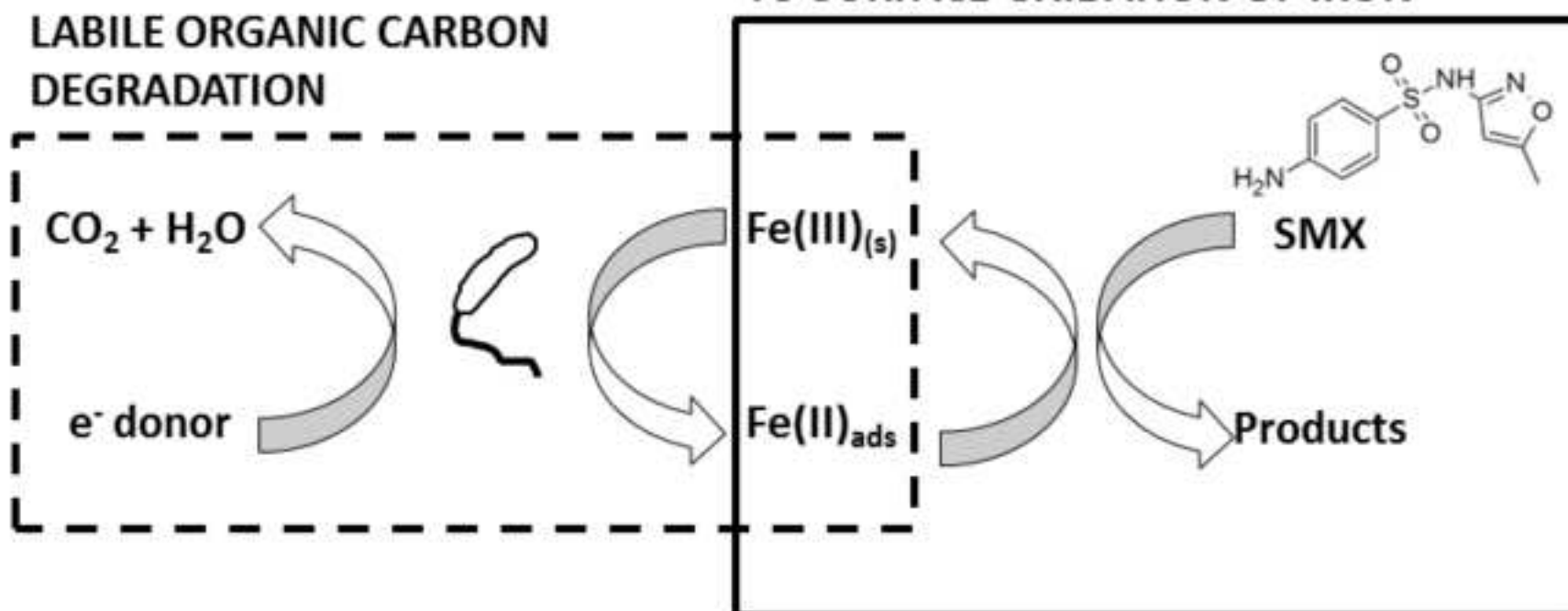
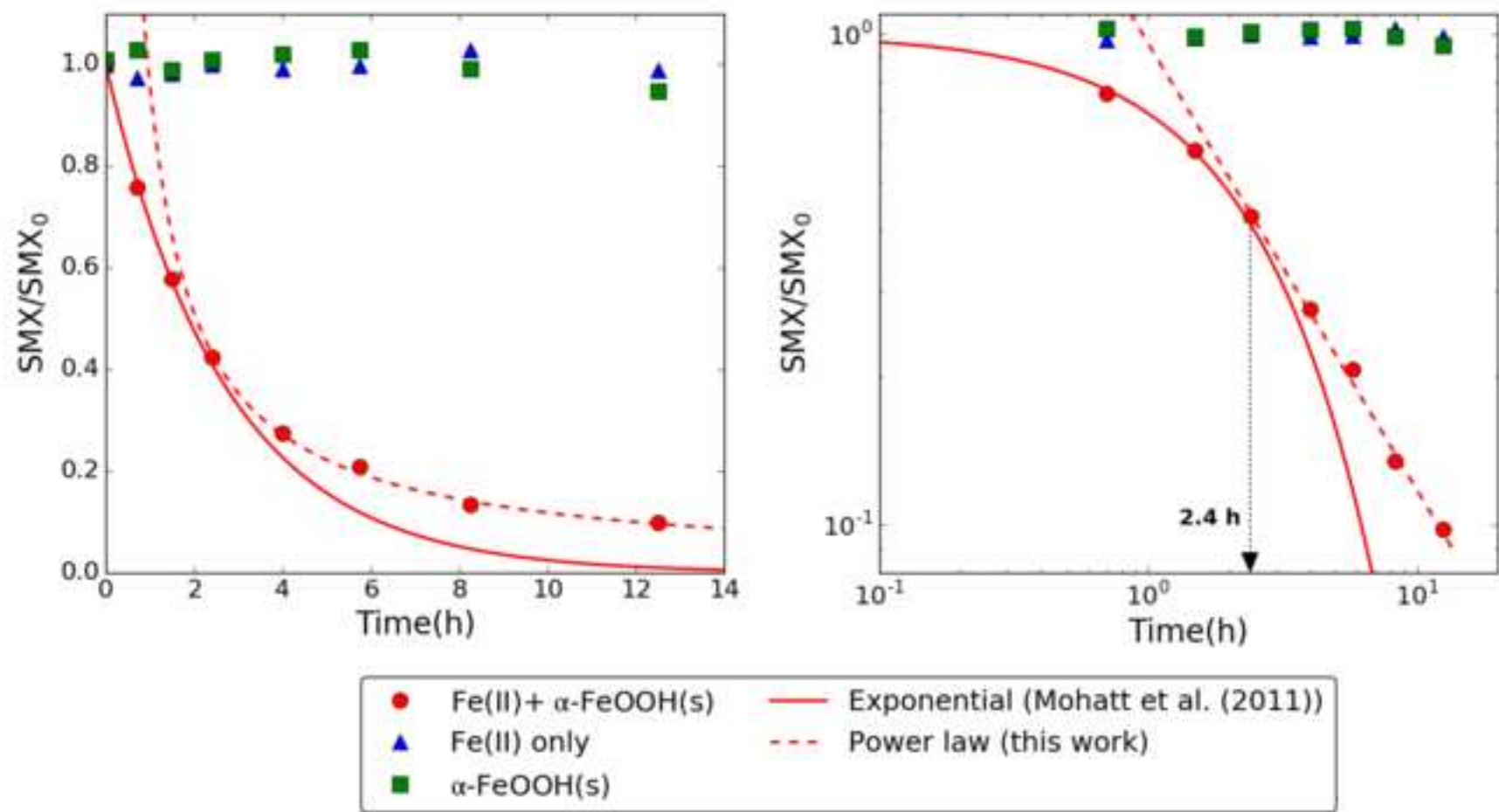


Figure5

[Click here to download high resolution image](#)



Electronic Supplementary Material (for online publication only)

[Click here to download Electronic Supplementary Material \(for online publication only\): SMX_supporting_information_v3.docx](#)